Electronic Supplementary Material (ESI) for Dalton Transactions.

"Synthesis and temperature-dependent studies of perovskite-like manganese formate framework templated by protonated acetamidine"

by Mirosław Mączka et al.

Table S1. Crystallographic data for AceMn.

	100(1) K	330(1) K
Empirical formula	$C_5H_{10}MnN_2O_6$	$C_5H_{10}MnN_2O_6$
Formula weight ($g \cdot mol^{-1}$)	249.09	249.09
Crystal system	monoclinic	orthorhombic
Space group	*P* $2_1/n$ (No 14)	*I mma* (No 74)
a (Å)	8.6727(11)	8.7482(2)
b (Å)	11.9317(13)	12.0885(3)
c (Å)	9.0332(12)	9.0317(2)
β (º)	92.233(14)	
V ($Å^3$)	934.1(2)	955.1(5)
Z	4	4
D_{calc} ($g \cdot cm^{-3}$)	1.771	1.732
μ (mm^{-1})	1.421	1.390
F(000)	508	508
Crystal size (mm)	0.21 × 0.20 × 0.19	0.21 × 0.20 × 0.19
Radiation type, λ (Å)	Mo *K*α , 0.71073	Mo *K*α , 0.71073
θ range(º)	2.83 ÷ 29.396	2.815 ÷ 29.543
Absorption correction	multi-scan	multi-scan
T_{min}/T_{max}	0.80827/ 1.000	0.89643 / 1.000
Refls collected / unique / observed	6100 / 2220 / 1438	20981 / 721 / 621

R_{int}	0.0303	0.0419
Refinement on	F^2	F^2
$R[F^2>2\sigma(F^2)]$	0.0487	0.0315
$wR(F^2$ all reflections)*	0.1013	0.0898
Goodness-of-fit, S	1.000	1.004
$\Delta\rho_{max}$, $\Delta\rho_{min}$ (e Å^{-3})	+1.322, -0.436	+ 0.478, -0.647

*$wR=\{\Sigma\,[w(F_o^2-F_c^2)^2]/\Sigma wF_o^4\}^{1/2}$; $w^{-1}=\sigma^2(F_o^2)+(aP)^2+(bP)$ where a=0.0321 and b=0 for 100(1) K and a= 0.0608 and b= 0.723 for 330(1) K, $P=(F_o^2+2F_c^2)/3$.

Table S2. Comparison of structural parameters for AceMn at 330 and 100 K, GuaMn at 293 K, FMDFe at 294 K, FMDMn at 355 and FMDMn at 110 K.

sample	AceMn[a]	AceMn[a]	GuaMn[b]	FMDFe[c]	FMDMn[d]	FMDMn[d]
	100 K	330 K	293 K	294 K	355 K	110 K
Space group	*P* $2_1/n$	*I mma*	*Pnna*	*Pnna*	*R-3c*	*C2/c*
a (Å)	8.6727	8.7482	8.5211	8.8246	8.8776	13.4375
b (Å)	11.9317	12.0885	11.9779	11.7336	8.8776	8.6838
c (Å)	9.0332	9.0317	9.0593	8.3258	19.5912	8.4075
β (º)	92.233	90	90	90	120	118.15
V (Å^3)	934.1	955.1	924.64	862.09	1337.2	865.0
Z	4	4	4	4	6	4
N···O distances (Å)	2.910-3.045	3.111-3.198	2.953-2.991	2.8883	2.8776	2.8570
				2.9340		2.8984
N-H···O angles (°)	164-175	137-159	160.3-169.1	173.2	167.0	170.0
				164.5		171.8
M···M distances (Å)	5. 9665	6.0445	5.989	5.8703	6.0772	6.0137
	6.1386	6.2869	6.219	6.0661		6.0435
	6.3824	6.2869	6.219	6.0661		
M-M-M angles (°)	87.658-92.327	88.173-91.827	86.493-93.507	86.668-	86.159	83.130-
				93.332	93.841	96.870
cis O-M-O angles (°)	84.39-101.88	86.78-93.22	81.65-106.12	85.35-98.20	86.36-93.64	85.45-94.55

[a]*This work;* [b]K.-L. Hu, M. Kurmoo, Z. Wang and S, Gao, *Chem. Eur. J*., 2009, **15,** 12050-12064, [c]A. Ciupa, M. Mączka, A. Gągor, A. Pikul, E. kucharska, J. Hanuza, A. Sieradzki, *Polyhedron,* 2015, **85,** 137-143, [d]M. Mączka, A. Ciupa, A. Gągor, A. Sieradzki, A. Pikul, B. Macalik and M. Drozd, *Inorg. Chem*., 2014, **53**, 5260-5268.

Table S3. IR and Raman wavenumebrs (in cm^{-1}) of AceMn and suggested assignments.[a]

Raman 400 K	Raman 80 K	IR 400 K	IR 80 K	Assignment
3356vw 3169vw	3309vw 3141m	3344m 3136m	3417sh 3325sh 3284m 3221m 3155m 3099m	νNH_2
	3033w 2989w 2941m	2945vw	3037vw 2991vw 2937vw	νCH_3
2865w	2891w	2866w	2893w 2872vw	νCH_3
2827m	2834s	2823m	2833m	$\nu_1 HCOO^-$
2708w	2717w 2702w	2710w	2750vw 2717w 2702vw	$2\nu_2 HCOO^-$
2124vw	2118vw			combinations
		1703s	1718sh 1713s	δNH_2
		1628sh	1672vw	νNCN
1579vw	1582vw	1595vs	1595vs	$\nu_4 HCOO^-$
1518w	1521w			νNCN
	1440w		1433w	δCH_3
1378sh 1371sh	1384m 1377m	1379m	1389m 1379m	$\nu_5 HCOO^-$
1358vs	1365 sh 1359vs	1356s	1367s 1360s 1353s	$\nu_2 HCOO^-$
	1354sh			
1349sh	1341vw			ρCH_3
1157w	1170w		1170vw	$\nu_{as} CCN$
	1148vw	1130w	1149w	ρNH_2
1064vw	1063vw		1061vw	$\nu_6 HCOO^-$
		1055vw	1057vw	ρCH_3
			1039vw	ρCH_3
893m	894m			$\nu_s CCN$

788w	796w	789s	795s	$\nu_3 HCOO^-$
		706m	742m 721m 685m	ωNH_2
534w	570vw 546w			τNH_2
462w	464w			δNCN
220vw	247vw 212vw			$T'HCOO^-$ $T'Mn^{2+}$
150m	176vw 163w 150m 140sh			$LHCOO^-$ $T'HCOO^-$
98m	118w 105m			$LHCOO^-$ T'Ace
78m	85w			$LHCOO^-$ LAce

[a]Key: s, strong; m, medium; w, weak; vw, very weak; sh, shoulder; b, broad

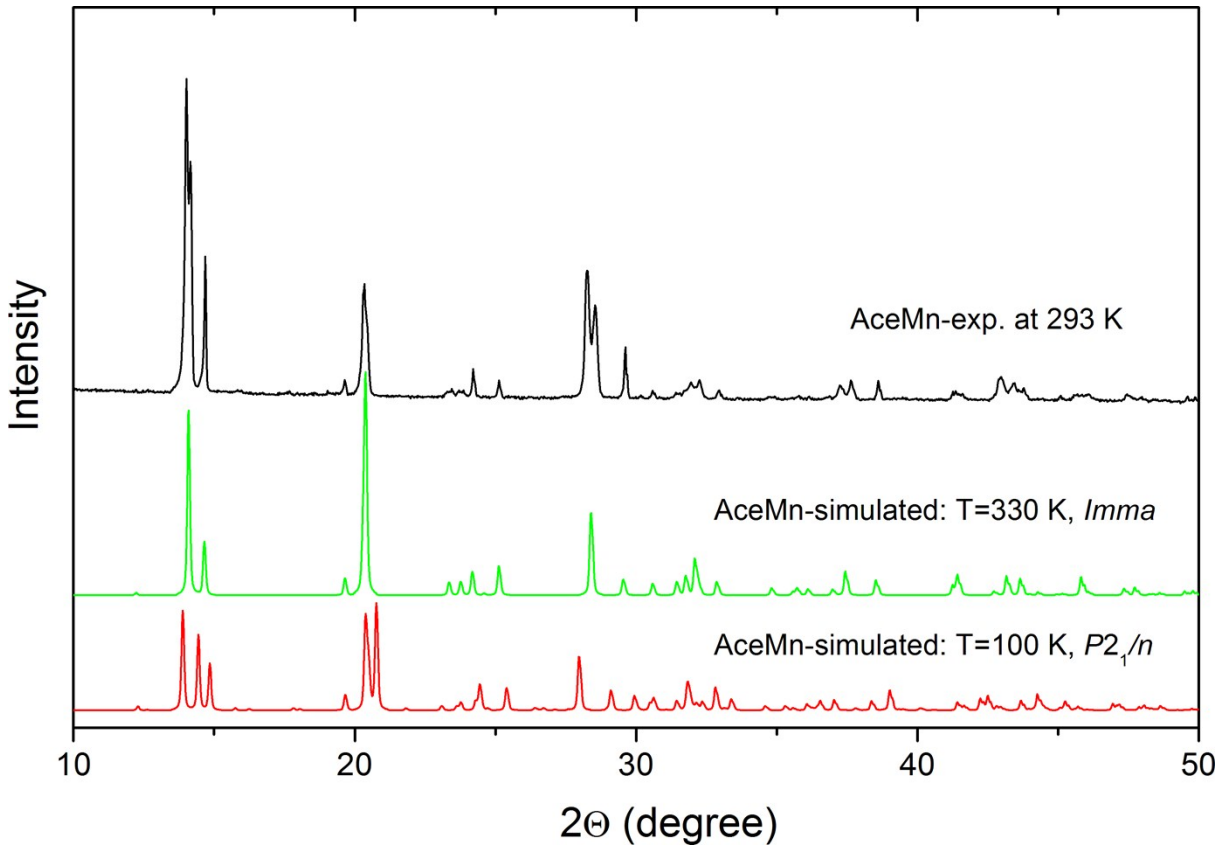

Figure S1. Room-temperature powder XRD pattern for the as-prepared sample together with the calculated ones based on the single crystal structures at 330 and 100 K. The experimental pattern is consistent with the monoclinic structure but splitting of the parent diffraction peaks of the orthorhombic phase is much less pronounced than expected at 100 K. This observation is constent with the fact that the experimental pattern was measured only 11 K below T_c=304 K.

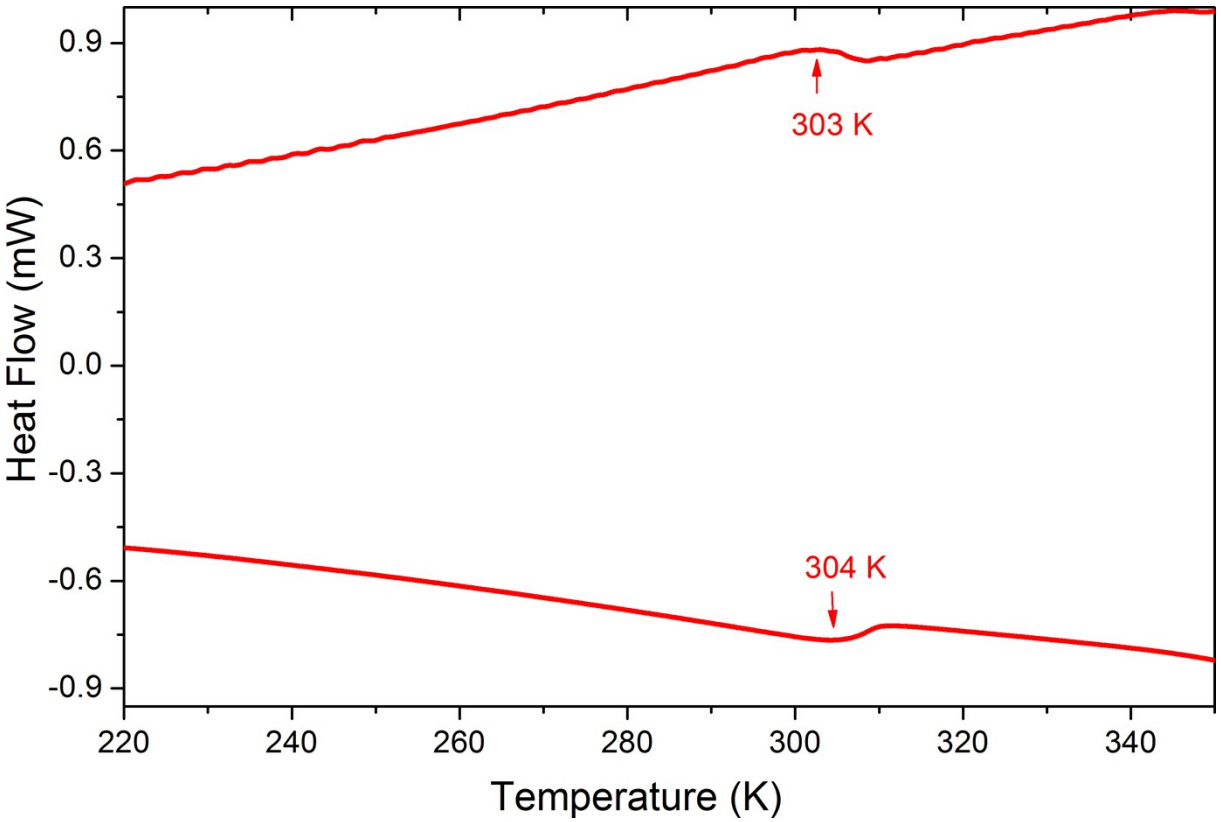

Figure S2. DSC traces for the prepared sample in heating and cooling modes.

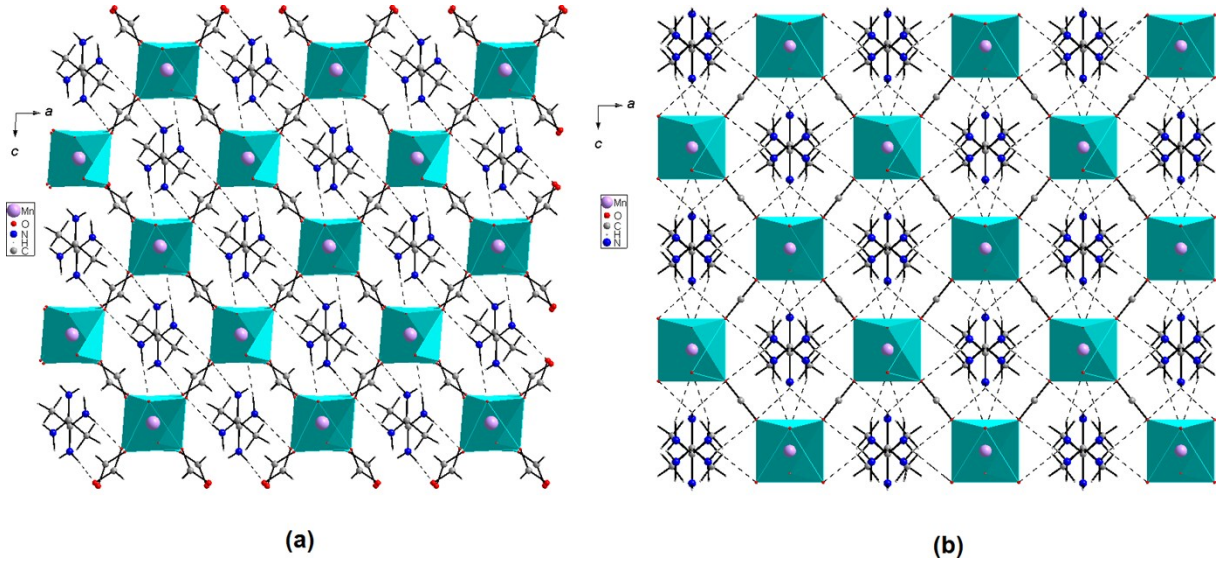

Figure S3. Projection of the anionic pseudo-perovskite Mn-formate framework together with the acetanidinium counter-ions in the cavities that interact via N-H···O hydrogen bonds in the (a) monoclinic and (b) orthorhombic modifications viewed along the *b* axis.

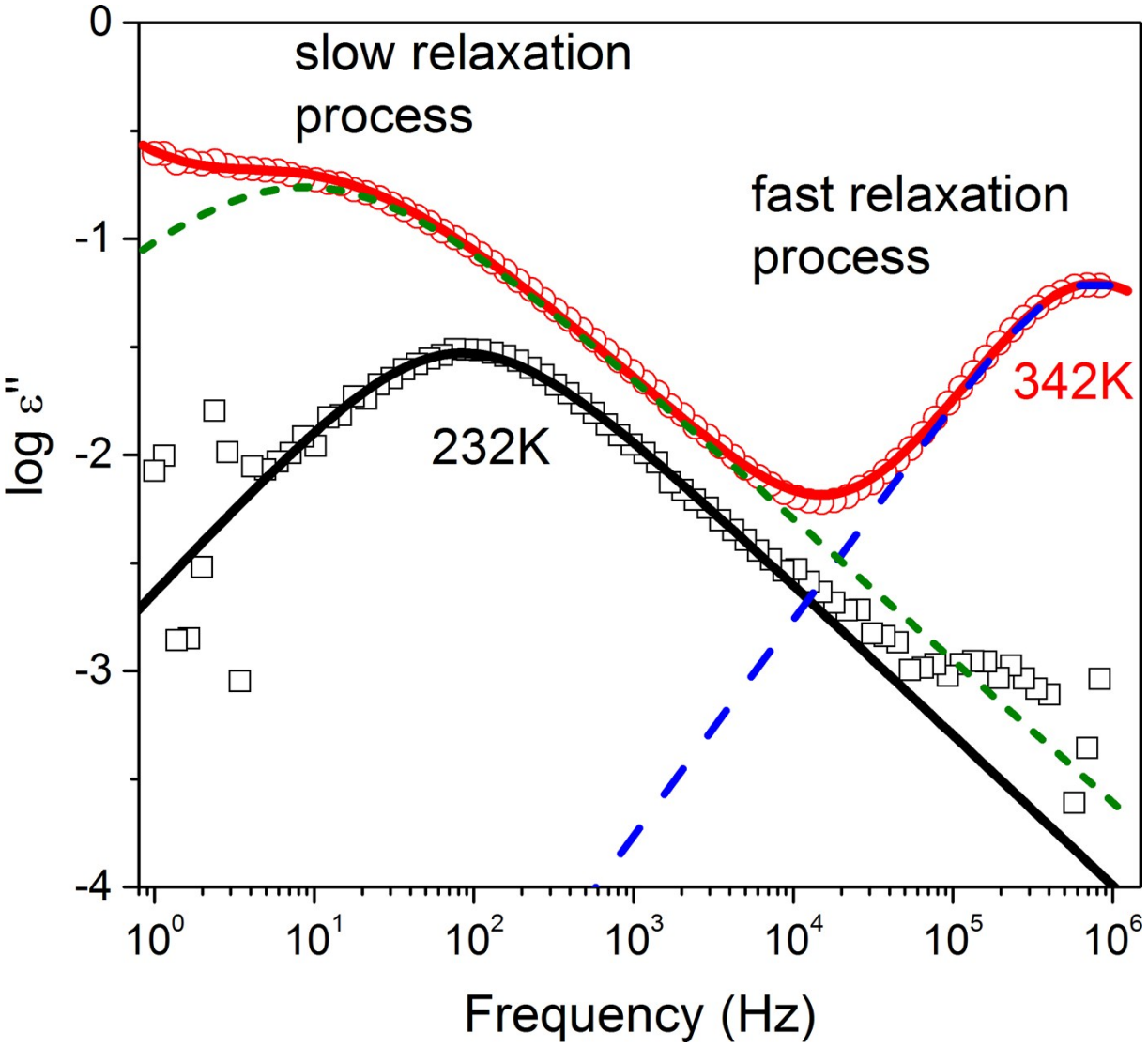

Figure S4. Isothermal dielectric loss spectra below (black squares) and above (red circles) phase transition temperature. Two dipolar relaxation processes were fitted by HN functions (solid and dash lines).

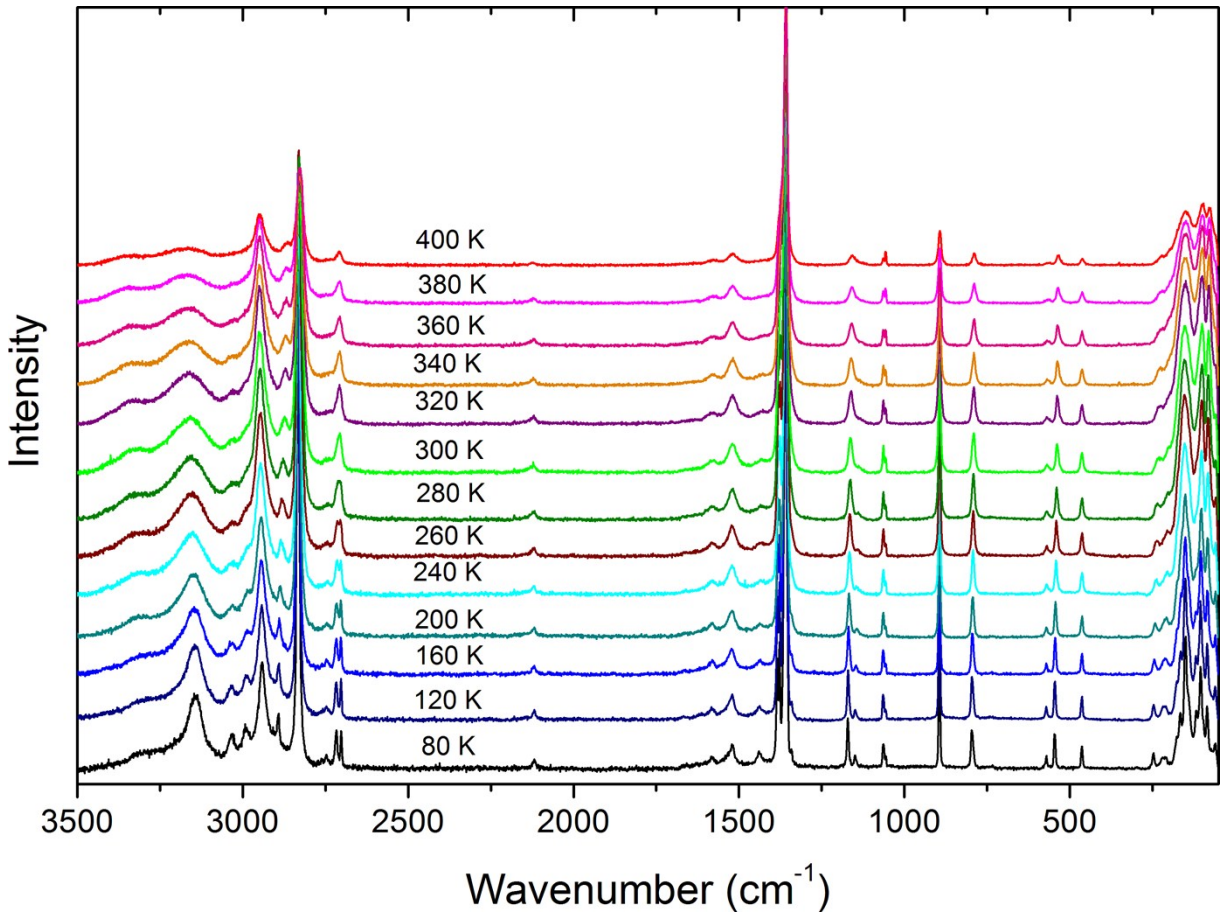

Figure S5. Temperature-dependent Raman spectra of AceMn in the 3500-50 cm^{-1} wavenumber range.

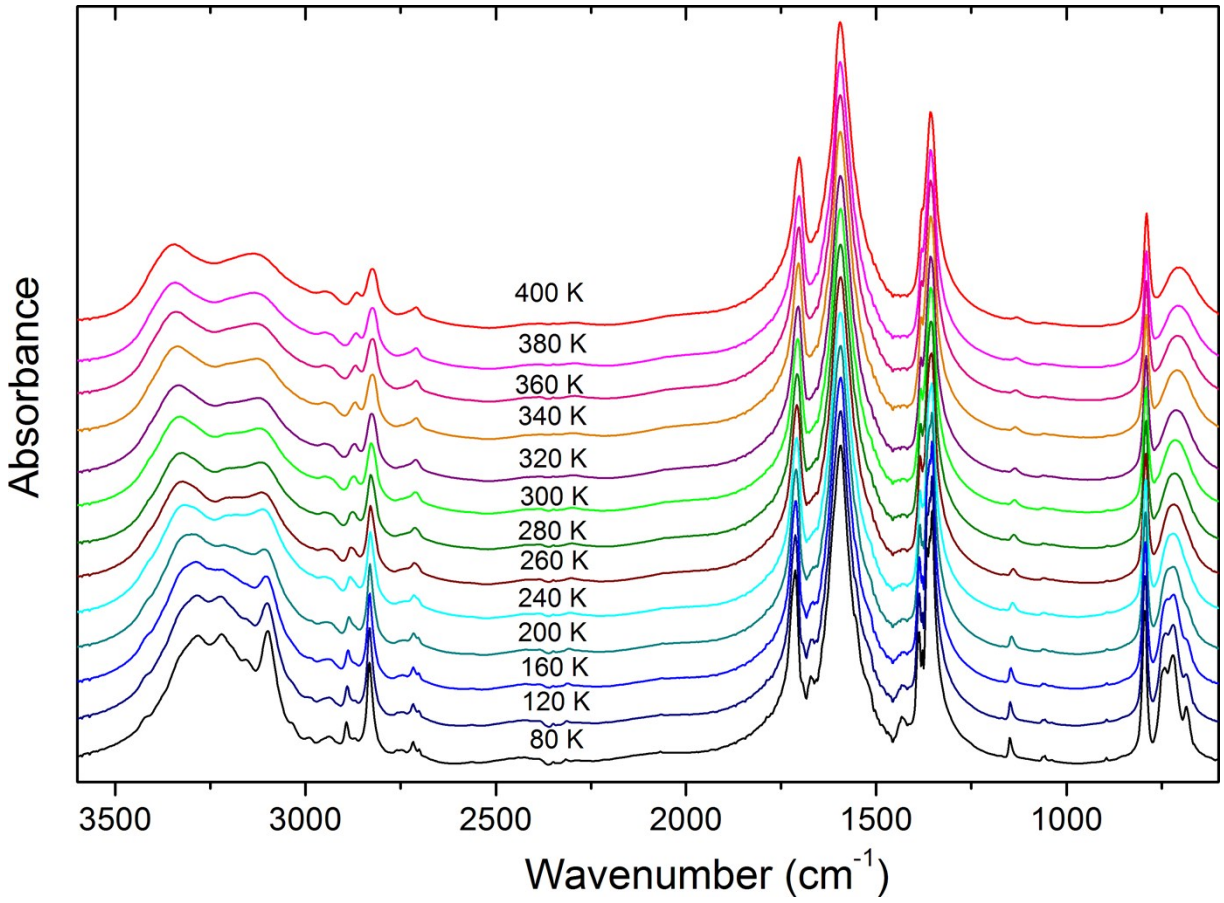

Figure S6. Temperature-dependent IR spectra of AceMn in the 3600-600 cm^{-1} wavenumber range.

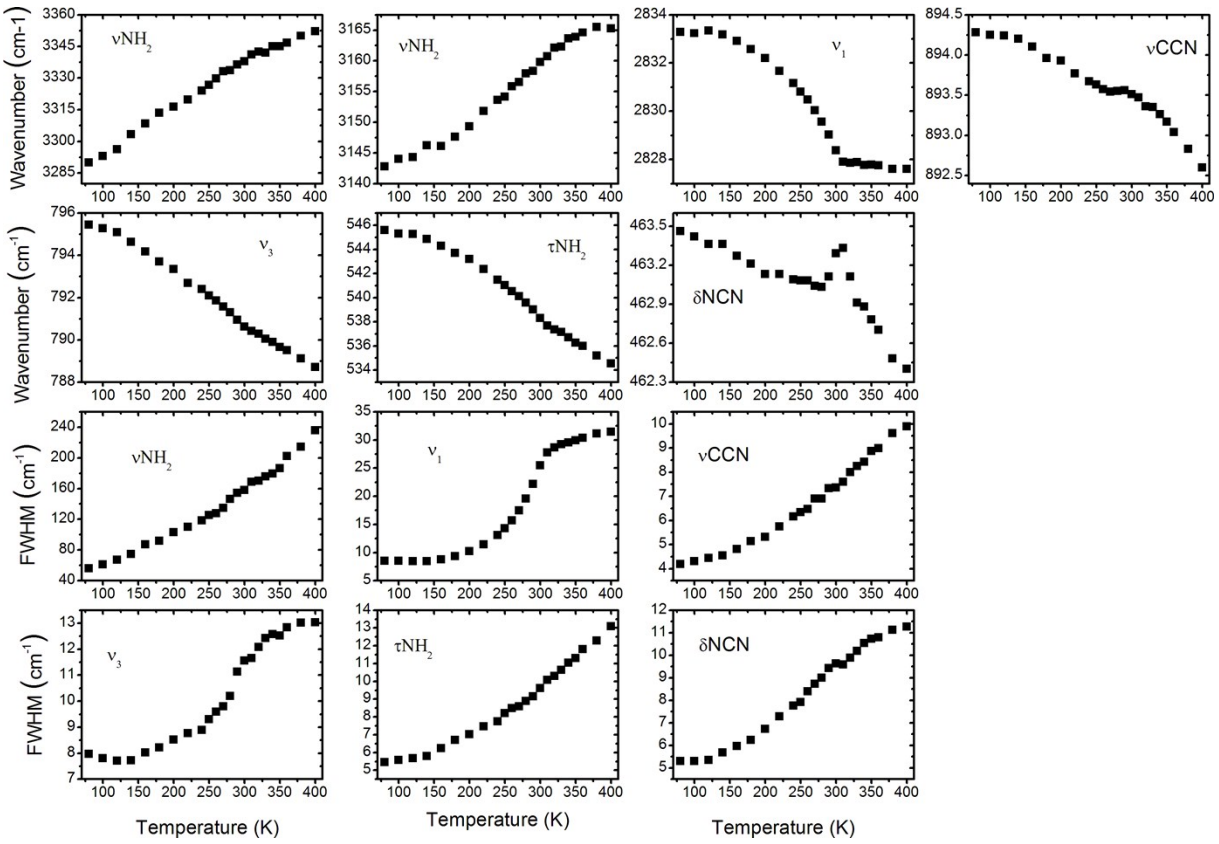

Figure S7. Temperature dependence of wavenumbers and FWHM for a few selected Raman-active modes of AceMn.